Aircraft Localization by Interacting Multiple Model Filtering in Wide Area Multilateration

Ludovico Mazzi*, Mattia Brambilla*, Michele Guardiani†, Maximilian James Arpaio†, Monica Nicoli*
*Politecnico di Milano, †Thales Italia S.p.A.

***Abstract*—Global air traffic has been steadily growing since the beginning of the new century, increasing the need for accurate and reliable positioning in real-time tracking of multiple aircrafts. This paper presents an Interacting Multiple Model (IMM) tracking solution and an assessment of a real Wide Area Multilateration (WAM) aircraft tracking scenario, where measurements from distributed Ground Stations (GSs) are gathered by a Central Processing Station (CPS) running the tracker. The assessment considers a main European airport, where a network of 44 GSs is used to monitor a congested area of 300 $\times$ 250 km. Tracking measurements refer to time differences of arrival (TDOAs) computed starting from the time of arrival (TOA) measured over downlink signals. Specifically, this work considers messages sent over the aviation transponder interrogation mode S. We present the results on IMM-based WAM tracking on airborne maneuvering targets, showcasing the improvements with respect to the conventional Automatic Dependent Surveillance - Broadcast (ADS-B) solution based on global navigation satellite systems (GNSSs).**

***Index Terms*—Air Traffic Control, Avionics, Interacting Multiple Model, MLAT, Localization, Surveillance, Tracking, WAM**

I. Introduction

The global air traffic demand is now recovering from the pandemic years with an increasing of 48.3% in the European area with respect to 2021 and a new record outlook is forecasted by the end of 2024 [1]. These facts call for an improvement of the capacity and performance of Air Traffic Management (ATM) system, while maintaining high safety criteria. The efforts in making air traffic safe, efficient and sustainable are relying on advanced monitoring technologies the Air Traffic Control (ATC) [2], [3]. Current technologies for avionics surveillance systems are divided into four distinct categories: Primary Surveillance Radar (PSR), Secondary Surveillance Radar (SSR), Automatic Dependant Surveillance - Broadcast (ADS-B), Multilateration (MLAT) [4]. Their combination ensures a reliable ATM. The PSR technology uses the radar echos reflected from the aircraft frame for positioning, resulting into an independent and non-cooperative surveillance system. Relying only on passive sensing, it does not require any equipment onboard the aircraft to support the operation, relying only on passive sensing. On the other hand, SSR is based on active transponders onboard the aircraft, which send reply messages upon interrogation by the ground-based surveillance system. In the ADS-B paradigm, the aircraft periodically broadcasts navigation information both to ATM ground systems and other airplanes [5]. The implementation of ADS-B relies on Global Navigation Satellite System (GNSS) to assess the aircraft position and an ADS-B transponder. Thus, ADS-B is labeled as a cooperative and dependent surveillance solution that can work alone or as a network of stations to improve performance [6]. Lastly, MLAT represents a cooperative and independent system, usually exploited as a backup method [7]. This technology uses standard aircraft transponder replies. The estimated positions is determined starting from the time of arrival (TOA) information received and processed by a network of fixed ground stations (GSs). MLAT can be integrated with ADS-B systems into a single station, yielding to easier and cheaper installations and maintenance. Within the same configuration, the MLAT technology is shown to be useful to assist ADS-B systems in recognizing malicious transmitted signals [8]. Furthermore, MLAT can withstand sparse malfunctioning or failure of the devices thanks to the large network of GSs used. Indeed, the performance of an MLAT-based system is comparable with traditional SSR solutions [9]. In addition, a recent study shows the feasibility for Wide Area Multilateration (WAM) to provide a backup surveillance technology independent of GNSS and capable of lightening the load on the already congested 1090 Mhz band, for instance by adopting LDACS system [10]. For all these reasons, the MLAT surveillance system is emerging as a suitable complement to well-established surveillance solutions [11].

The analysis of the Geometric Dilution of Precision (GDOP) of MLAT outlines the severe degradation on the vertical accuracy due to the Earth-based locations of GSs. In [12], the authors investigate an approach based on a stochastic constellation of available receivers which varies in time and accounts for changes in signal detection capability. To enhance the accuracy on the vertical dimension, the use of barometric altitude information has been conceived [13], often aided by altitude correction error mitigation methods [14].

Within the MLAT framework, tracking algorithms play a fundamental role. Throughout flights, guidance and position estimation models enable certain crucial aspects, i.e., air space separation and aircraft monitoring [15]. These solutions find application also in ATC decision support tools and provide augmented capabilities also in critical conditions, such as collision warning and avoidance systems [16]. Several aircraft tracking strategies have been proposed in the literature, most of them relying on stochastic methods exploiting the dynamics of the target and the measurement uncertainty [17]–[19]. Other approaches relying on Extended Kalman Filter (EKF) and decision-based methods have been proposed as well [20], [21]. An efficient aircraft tracking solution is the Interacting

Multiple Model (IMM) [22]. The IMM tracker rooted in [23], and further developed in [24]. The IMM relies in multiple filters running in parallel and outputs a weighted estimation of the related estimates. It represents a suitable answer to the need of augmentation of performance with relatively low computational complexity. The main characteristic of this algorithm lies in its capacity of predicting the state of a dynamic system subject to several behaviours, by the interaction of multiple motion models. In addition, IMM is adaptable: it can be implemented using as building components Kalman Filters (KFs), EKFs, Unscented Kalman Filters (UKFs), possibly combined with particle filters or other advanced solutions [25]. An example in this direction is the Interacting Multiple Model Particle Filter (IMM-PF) [26]. However, this solution suffers from a high computational complexity and therefore it should be avoided for real-time tracking scenarios. For this reason, in this work we consider an EKF-based implementation of IMM to real-time aircraft tracking.

The contribution of the present work is the development and assessment of an IMM-based tracking solution for ATC relying on a network of ground-based distributed stations. The positioning algorithm is designed to track maneuvering aircrafts in a real WAM scenario. Though the proposed algorithm is cooperative, it does not require solving a data association problem [27]–[33] as WAM systems use Mode S messages [34]. Being the target aircraft interrogated and forced to transmit a specific signal, the ambiguity of association is minimized. The downlink signal is received by the GSs, which forward the TOA information to a Central Processing Station (CPS), allowing coherent cooperative processing. We propose to compute time difference of arrival (TDOA) measurements exploiting an IMM-based EKF. Attention is paid on the use of real data and the need for measurement filtering to remove unreliable measurements (i.e., outliers).

This paper is structured as follows. Section II presents the problem formulation of a WAM aircraft tracking scenario. Section III provides the mathematical derivation of the solution to the tracking problem by describing the EKF and IMM working principles. Section IV describes the experimental layout, the adopted technology, and present experimental results. Concluding remarks are drawn in Section V.

II. Problem Formulation

We address the problem of tracking maneuvering air targets from a network of M GSs in the WAM scenario illustrated in Fig. 1. Aircrafts follow routes designated by governmental institutions and aviation safety agencies [35], while real-time tracking of their positions is managed by ATC centers for surveillance. To this aim, we investigate the use of MLAT technologies. The message are processed by each GS within the cooperative network to estimate the associated TOA. The TOA information is then sent to the CPS, where TDOA computation takes place. The use of TDOAs instead of TOAs allows to minimize synchronization issues between aircrafts and ground receivers, and also to mitigate the effects of

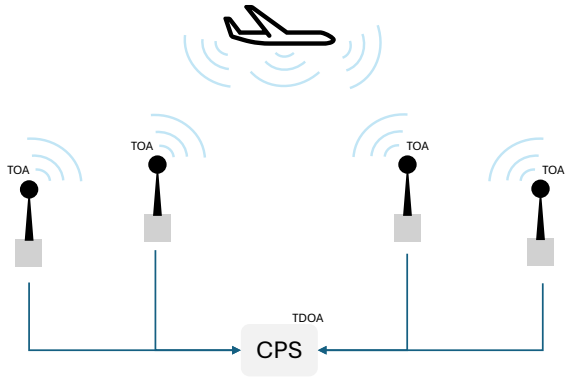

Fig. 1. Illustration of the considered WAM scenario, where GSs forward the TOA measurement to a CPS in charge of aircraft localization with TDOAs.

multipaths. The TDOA measurements constitute the input source for localizing the associated aircraft.

The 3-D coordinate of the m-th GS, $m = 1, \ldots, M$, is denoted with $\mathbf{p}_m = [p_{m,x}\, p_{m,y}\, p_{m,z}]$, while the state of the aircraft at time instant t is indicated with $\mathbf{x}_t$ and is defined according to the motion model used for tracking. In this work, the following aircraft kinematic models are considered: a Nearly-Constant Velocity (NCV), a Nearly-Constant Acceleration (NCA) (specifically, the Wiener-sequence acceleration model [36]) and a horizontal Constant Turn Rate (CTR) plus NCV for the elevation direction (simply referred as CTR throughout all the manuscript). Depending on the specific model, it can include 3-D position $\mathbf{u}_t = [u_{x,t}, u_{y,t}, u_{z,t}]^{\mathrm{T}}$, 3-D velocity $\mathbf{v}_t = [v_{x,t}, v_{y,t}, v_{z,t}]^{\mathrm{T}}$, 3-D acceleration $\mathbf{a}_t = [a_{x,t}, a_{y,t}, a_{z,t}]^{\mathrm{T}}$ or horizontal turn rate $\omega_{xy,t}$. As a result, the associated states for the NCV, NCA and CTR are given by:

$$\mathbf{x}_t^{\mathrm{NCV}} = [u_{x,t}\, u_{y,t}\, u_{z,t}\, v_{x,t}\, v_{y,t}\, v_{z,t}]^{\mathrm{T}}, \tag{1}$$

$$\mathbf{x}_t^{\mathrm{NCA}} = [u_{x,t}\, v_{x,t}\, a_{x,t}\, u_{y,t}\, v_{y,t}\, a_{y,t}\, u_{z,t}\, v_{z,t}\, a_{z,t}]^{\mathrm{T}}, \tag{2}$$

$$\mathbf{x}_t^{\mathrm{CTR}} = [u_{x,t}\, v_{x,t}\, u_{y,t}\, v_{y,t}\, u_{z,t}\, v_{z,t}\, \omega_{xy,t}]^{\mathrm{T}}. \tag{3}$$

The reply-to-interrogation signal sent by the aircraft and received by the GSs is used to estimate the TOA. The TOA measurement available at GS m at time t is defined by:

$$\rho_{m,t} = \frac{||\mathbf{p}_m - \mathbf{u}_t||_2}{c} + n_{m,t}, \tag{4}$$

where $n_{m,t}$ indicates an additive noise term, while c is the propagation speed. Then, the TOA measurements are aggregated by a CPS, which converts them into TDOA information. The TDOA measurement between the pair (m, n) of GSs at time t is defined as:

$$z_{m,n,t} = \rho_{m,t} - \rho_{n,t}, \quad \forall\, m, n = 1, \ldots, M, m \neq n. \tag{5}$$

All the available TDOA measurements at time t are stacked in the aggregated vector $\mathbf{z}_t$, which is used for tracking. Note that the multipath effects degrade the reliability of TDOAs and, together with synchronization errors between GSs, Signal-to-Noise Ratio (SNR) of the signals and GDOP of GS deployment, affect the overall accuracy of the MLAT system. Under

these circumstances, designing and implementing filtering and tracking algorithms become imperative for an effective solution. Note that the indexes of the measurement in $\mathbf{z}_t$ are univocally mapped to the originating GS, thus allowing the implementation of an EKF, as described in the next section.

III. Aircraft tracking algorithm

This section presents the mathematical formulation of the developed IMM-based EKF for aircraft tracking in a WAM system. First, the EKF is described (Section III-A), with emphasis on the definition of residual (or innovation), then the IMM algorithm is explained (Section III-B).

A. Extended Kalman filter

The vector of TDOA measurements $\mathbf{z}_t$ is used within an EKF for tracking the aircraft maneuvers. Specifically, an IMM implementations foresees multiple EKFs running in parallel, each with a specific motion model (NCV, NCA, CTR). We denote the state estimate at time t of the i-th motion model as $\mathbf{x}_{t|t}^{(i)}$, while $\mathbf{P}_{t|t}^{(i)}$ indicates its covariance. The EKF amounts to recursively estimate the state mean and covariance over time. This implies a prediction step, where the motion model describes the transition from $t-1$ to t (the time interval is indicated with ΔT) and is used to get an a-priori knowledge at time t as:

$$\mathbf{x}_{t|t-1}^{(i)} = \mathbf{F}^{(i)}\mathbf{x}_{t-1|t-1}^{(i)}, \tag{6}$$

$$\mathbf{P}_{t|t-1}^{(i)} = \mathbf{F}^{(i)}\mathbf{P}_{t-1|t-1}^{(i)}\mathbf{F}^{(i)^{\mathrm{T}}} + \mathbf{Q}^{(i)}, \tag{7}$$

where the matrices $\mathbf{F}^{(i)}$ and $\mathbf{Q}^{(i)}$ univocally depend on the motion model and its characterization (see Table I).

After the prediction phase, the TDOA measurements $\mathbf{z}_t$ are used to correct the a-priori information, both in terms of mean shift and covariance reduction. The correction phase requires the linearization of TDOA measurements around the state prediction. To this extent, a properly-defined observation matrix $\mathbf{H}_t^{(i)}$ is used, whose structure and dimension depend on the state, i.e., on the considered motion model and number of available measurements. The measurements residual (or innovation) $\mathbf{r}_t^{(i)}$ is calculated as:

$$\mathbf{r}_t^{(i)} = \mathbf{z}_t - \mathbf{H}_t^{(i)}\mathbf{x}_{t|t-1}^{(i)}, \tag{8}$$

while the innovation covariance is:

$$\mathbf{S}_t^{(i)} = \mathbf{H}_t^{(i)}\mathbf{P}_{t|t-1}^{(i)}\mathbf{H}_t^{(i)^{\mathrm{T}}} + \mathbf{R}_t, \tag{9}$$

being $\mathbf{R}_t$ the covariance matrix of all the available TDOA measurements, constructed from the noise term in (4). Lastly, by defining the so-called Kalman gain $\mathbf{G}_t^{(i)}$ as:

$$\mathbf{G}_t^{(i)} = \mathbf{P}_{t|t-1}^{(i)}\mathbf{H}_t^{(i)^{\mathrm{T}}}\left(\mathbf{S}_t^{(i)}\right)^{-1}, \tag{10}$$

the updated state estimate representing the aircraft state at time t is:

$$\mathbf{x}_{t|t}^{(i)} = \mathbf{x}_{t|t-1}^{(i)} + \mathbf{G}_t^{(i)}\mathbf{r}_t^{(i)}, \tag{11}$$

$$\mathbf{P}_{t|t}^{(i)} = \mathbf{P}_{t|t-1}^{(i)} - \mathbf{G}_t^{(i)}\mathbf{S}_t^{(i)}\mathbf{G}_t^{(i)^{\mathrm{T}}}. \tag{12}$$

Notice that the Kalman gain is the core aspect of the filter, as it weights the prediction against the correction.

B. Interacting multiple model

The IMM algorithm relies on a probabilistic-based fusion of the tracking results from multiple EKFs. Specifically, the individual state estimates of each model, i.e., $\mathbf{x}_{t|t}^{(i)}$ and $\mathbf{P}_{t|t}^{(i)}$, are combined to obtain a single output estimate for each time instant t. To do that, a weighting operation is done, where each motion model is associated to a model probability $\mu_{t|t}^{(i)}$, representing the likelihood that the model i is well matching the observed kinematic transition. The final state estimate at the output of the IMM is computed as:

$$\mathbf{x}_{t|t} = \sum_{i=1}^{N_{\mathrm{M}}} \mu_{t|t}^{(i)}\,\mathbf{x}_{t|t}^{(i)}, \tag{13}$$

$$\mathbf{P}_{t|t} = \sum_{i=1}^{N_{\mathrm{M}}} \mu_{t|t}^{(i)}\left(\mathbf{P}_{t|t}^{(i)} + \left(\mathbf{x}_{t|t}^{(i)} - \mathbf{x}_{t|t}\right)\left(\mathbf{x}_{t|t}^{(i)} - \mathbf{x}_{t|t}\right)^{\mathrm{T}}\right), \tag{14}$$

where N_{M} indicates the overall number of multiple models.

The evolution of IMM probabilities follows a *prediction-correction* approach over time, as for the EKF. Specifically, the IMM also foresees the definition of the switching probability p_{ij}, modeling the transition from model i to j (if $i = j$ it enforces staying on the same model). The impact of p_{ij} is a correction of the model probability while transitioning from time $t-1$ to time t. The probability $\mu_{t-1||t-1}^{(i)}$ is modified as:

$$\mu_{t|t-1}^{(i)} = \sum_{j=1}^{N_{\mathrm{M}}} p_{ij}\,\mu_{t-1|t-1}^{(j)}, \tag{15}$$

where $\mu_{t|t-1}^{(i)}$ can be interpreted as a predicted model likelihood, i.e., an indication of how likely a given model will be in the forthcoming observation time instant.

The predicted model likelihood is then updated with the information coming from the current measurements $\mathbf{z}_t$ and embedded into the innovation term (8). This correction is modeled by $\Lambda_t^{(i)}$ defined as:

$$\Lambda_t^{(i)} = \mathcal{N}\left(\mathbf{r}_t^{(i)}; 0, \mathbf{S}_t^{(i)}\right). \tag{16}$$

Lastly, from (15) and (16), the updated model probability at time t is obtained as:

$$\mu_{t|t}^{(i)} = \frac{\mu_{t|t-1}^{(i)}\Lambda_t^{(i)}}{\sum_{j=1}^{N_{\mathrm{M}}}\mu_{t|t-1}^{(j)}\Lambda_t^{(j)}}. \tag{17}$$

IV. Experimental results

This section presents the assessment of the IMM-based EKF for aircraft tracking in a real WAM system. First, Section IV-A describes the overall surveillance system and its technology. Then, we discuss about implementation aspects in Section IV-B. Lastly, the evaluation of tracking performance is presented in Section IV-C.

TABLE I
DEFINITION OF MOTION MODEL-DEPENDENT MATRICES

	NCV	NCA	CTR
$\mathbf{F}^{(i)}$	$\mathbf{I}_3 \otimes \begin{bmatrix} 1 & \Delta T \\ 0 & 1 \end{bmatrix}$	$\mathbf{I}_3 \otimes \begin{bmatrix} 1 & \Delta T & \frac{\Delta T^2}{2} \\ 0 & 1 & \Delta T \\ 0 & 0 & 1 \end{bmatrix}$	$\begin{bmatrix} 1 & TS & 0 & -TC & 0 & 0 & 0 \\ 0 & \cos(\omega_{xy,t}\Delta T) & 0 & -\sin(\omega_{xy,t}\Delta T) & 0 & 0 & 0 \\ 0 & TC & 1 & TS & 0 & 0 & 0 \\ 0 & \sin(\omega_{xy,t}\Delta T) & 0 & \cos(\omega_{xy,t}\Delta T) & 0 & 0 & 0 \\ 0 & 0 & 0 & 0 & 1 & \Delta T & 0 \\ 0 & 0 & 0 & 0 & 0 & 1 & 0 \\ 0 & 0 & 0 & 0 & 0 & 0 & 1 \end{bmatrix}$
$\mathbf{Q}^{(i)}$	$\sigma_w^{\mathrm{NCV}^2} \mathbf{I}_3 \otimes \begin{bmatrix} \frac{\Delta T^4}{4} & \frac{\Delta T^3}{2} \\ \frac{\Delta T^3}{2} & \Delta T^2 \end{bmatrix}$	$\sigma_w^{\mathrm{NCA}^2} \mathbf{I}_3 \otimes \begin{bmatrix} \frac{\Delta T^4}{4} & \frac{\Delta T^3}{2} & \frac{\Delta T^2}{2} \\ \frac{\Delta T^3}{2} & \Delta T^2 & \Delta T \\ \frac{\Delta T^2}{2} & \Delta T & 1 \end{bmatrix}$	$\mathrm{diag}\left(\sigma_w^{\mathrm{NCV}^2} \mathbf{I}_3 \otimes \begin{bmatrix} \frac{\Delta T^4}{4} & \frac{\Delta T^3}{2} \\ \frac{\Delta T^3}{2} & \Delta T^2 \end{bmatrix}, \sigma_w^{\mathrm{CTR}^2} \Delta T^2 \right)$

For the CTR model, the following variables are used: $TS = \frac{\sin(\omega_{xy,t}\Delta T)}{\omega_{xy,t}}$, $TC = \frac{1-\cos(\omega_{xy,t}\Delta T)}{\omega_{xy,t}}$.

A. WAM surveillance system

We consider a WAM system with $M = 44$ GSs, distributed over a region of 300 $\times$ 250 km around a main European airport. The GS positions with respect to a local reference frame centered at the airport (located at [0,0] km) are represented in Fig. 2, where we point out a higher density around the airport. The effect of geometry associated to the WAM scenario under investigation is illustrated in Fig. 3 in terms of horizontal GDOP at 1000 m.

WAM surveillance exploits Mode S messages sent by aircrafts upon interrogation from GSs. Namely, GSs query the aircraft with uplink messages at 1030 MHz, which replies with the requested information. The downlink signal is at 1090 MHz, and it is used to estimate the TOA by extracting the delay related to the first peak of the cross-correlation between the received signal and local replica of the transmitted signal. The downlink message including a preamble plus 112 bits of data, it has a Manchester encoding scheme facilitating the bit error detection. Pulse amplitude modulation (PPM) is used. For each receiving GS, the signal is down-converted to baseband and demodulated to decode the entire message. Then, all the GSs forward their message to the CPS, where data are processed. These data representing TOAs are then combined to obtain TDOA information. The collected Mode S data refer to traffic of opportunity, gathered at variable frequencies, typically around 2 Hz. Notice that, the availability of measurements at each GS is not periodic, as there are factors related to signal propagation that might prevent the reception. As a result, the availability of measurements is intermittent and non-periodic, also characterized by outliers. The implementation of the IMM-based EKF intrinsically accounts for such aperiodicity with the variable time interval ΔT, as well as with the subset of active GSs (i.e., those producing a reliable TOA measurement) by dynamically adjusting the matrices $\mathbf{H}_t^{(i)}$ and $\mathbf{R}_t^{(i)}$.

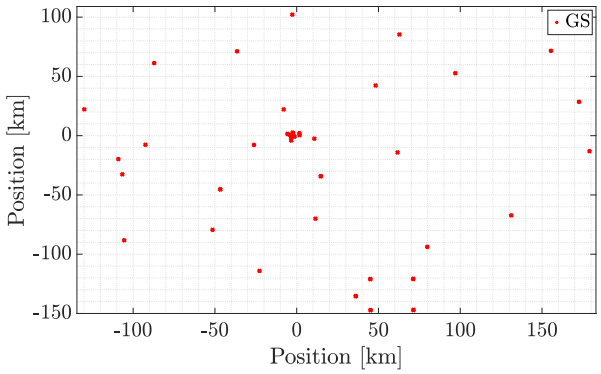

Fig. 2. Positions of the GSs over the region of interest (with respect to the local reference frame centered at the airport).

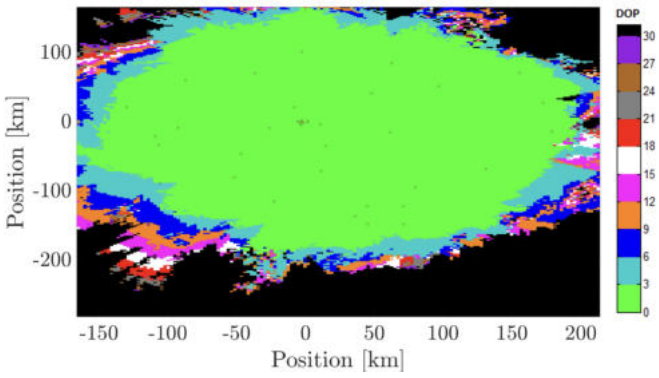

Fig. 3. Horizontal GDOP for the considered WAM scenario at 1000 m altitude, with red crosses representing the GSs.

B. Positioning filter settings

For each EKF, the covariance $\mathbf{Q}^{(i)}$ (defined in Table I) of the state transition model is calibrated to adapt to the different aircraft dynamics. The resulting values of standard deviation are: $\sigma_w^{\mathrm{NCV}} = 0.8$ m/s^2, $\sigma_w^{\mathrm{NCA}} = 0.1$ m/s^3, $\sigma_w^{\mathrm{CTR}} = 1$ deg/s^2.

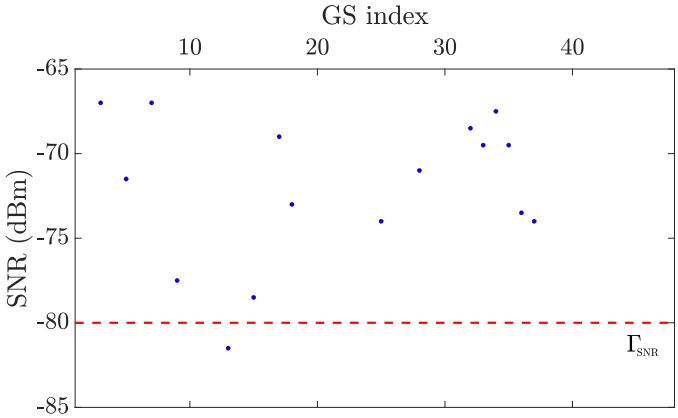

Fig. 4. Example for one time interval of outlier identification based on SNR threshold value. The dots indicate the value of SNR associated to the available GSs, the red dashed line is the threshold. In this case, one measurement is discarded.

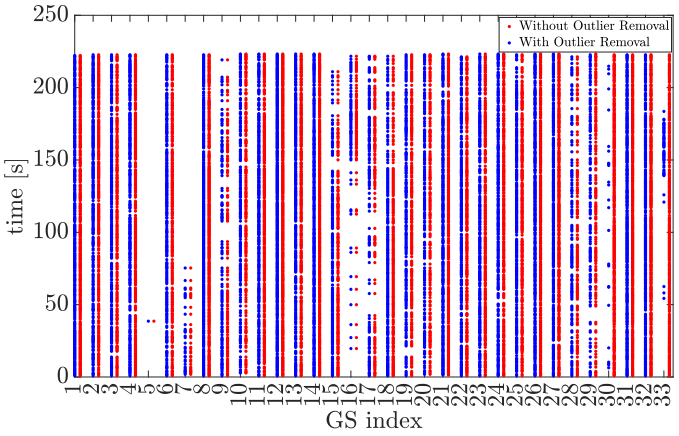

Fig. 5. TOA availability for each involved GS over tracking time. A single dot indicates the presence of a TOA measurement. The measurement availability is compared for the case with (red) or without (blue) the outliers.

Concerning the localization measurements, we assume the TDOA to be independent across the GSs, resulting into a diagonal covariance matrix $\mathbf{R}_t$ with entries on the main diagonal equal to 112.5 m^2. This value comes from analyses of the GS synchronization, which show an accuracy on TOA of 25 ns.

Regarding the IMM, the initialization assumes the same model probability for the three considered motion models, i.e., $\mu_{0|0}^{(i)} = 33\%$, while, by picking istances from the literature [37], the transition probabilities are specified as:

$$p_{ij} = \begin{cases} 0.95 & i = j, \\ 0.025 & i \neq j. \end{cases} \tag{18}$$

For identifying and removing unreliable measurements, we proceed with two consecutive strategies, described in the following. Since the Mode S message contains the value of SNR (expressed in dBm), we use this information for a first identification of poor quality measurements. Denote with $\text{SNR}_{m,t}$ the SNR value associated to the measurement $\rho_{m,t}$, and with Γ_{SNR} an SNR threshold. If $\text{SNR}_{m,t} < \Gamma_{\text{SNR}}$, it is likely that the TOA $\rho_{m,t}$ is unreliable. Thus, we account for this issue increasing the associated noise variance term by a factor of 2. The SNR threshold is set to -80 dBm. An example of such SNR-based outlier identification strategy is reported in Fig. 4.

The second strategy for handling possible outliers refers to the inspection of the residuals in (8). Also in this case, a threshold-based analysis is carried out. Denote the residual threshold as Γ_{r}. If the absolute value of the single entry of $\mathbf{r}_t$ exceeds Γ_{r}, the TOA of the GS non considered as reference for the TDOA computation is discarded.

An example on the effect of removing outlier is represented in Fig. 5, where we analyze the measurement availability for each involved GS in tracking one aircraft, comparing the measurement availability with (blue) and without (red) the outlier removal. On average, 8.1% of measurements is removed. If the two strategies discard all the available measurements, the EKF works in a prediction-only condition, with $\mathbf{x}_{t|t} = \mathbf{x}_{t|t-1}$ and $\mathbf{P}_{t|t} = \mathbf{P}_{t|t-1}$. In this case, the merged model probabilities $\mu_{t|t-1}^{(i)}$ are updated inward with (17).

C. Performance evaluation

We evaluate the performance of the EKF-based IMM for aircraft tracking by WAM against ADS-B positioning. Indeed, together with the Mode S messages, we recorded the positions broadcasted by the ADS-B transponder.

We focus the analyses on two selected real aircraft trajectories. The first track involves both linear and turning movements, while the second one refers to turning maneuver followed by a straight motion. The localization performance for the first trajectory is shown in Fig. 6 in terms of 2-D location fixes over the horizontal plane. The focus of the analysis is a comparison of the proposed IMM-based EKF tracker (blue curve) with respect to the ADS-B positioning technology (dashed green curve), for both the cases of neglecting (Fig. 6a) or not (Fig. 6b) the outlier mitigation strategies. From the tracks in Figs. 6a-6b, we observe the need of implementing an outlier detection and correction mechanism to successfully track the target. Indeed, only by discarding unreliable measurements we manage to reconstruct a reliable aircraft trajectory, that attains the ADS-B positioning (Fig. 6b).

The second aircraft trajectory is characterize by a turning maneuver lasting approximately 20 s, followed by a straight motion. In Fig. 7 we analyze the tracking performance of the EKF-IMM tracker with and without outlier removal. Top row of the figure considers the case of ignoring the presence of outliers and represents the localization performance against the ADS-B in terms of 2-D estimated aircraft trajectory (Fig. 7a), speed (Fig. 7b) and acceleration (Fig. 7c). Bottom row instead considers the EKF-IMM implementation with outlier removal, for the same analyses on trajectory (Fig. 7d), speed (Fig. 7e) and acceleration (Fig. 7f). Note that the aircraft speed and acceleration for the ADS-B solution are obtained by differentiating the position estimates. We also represent

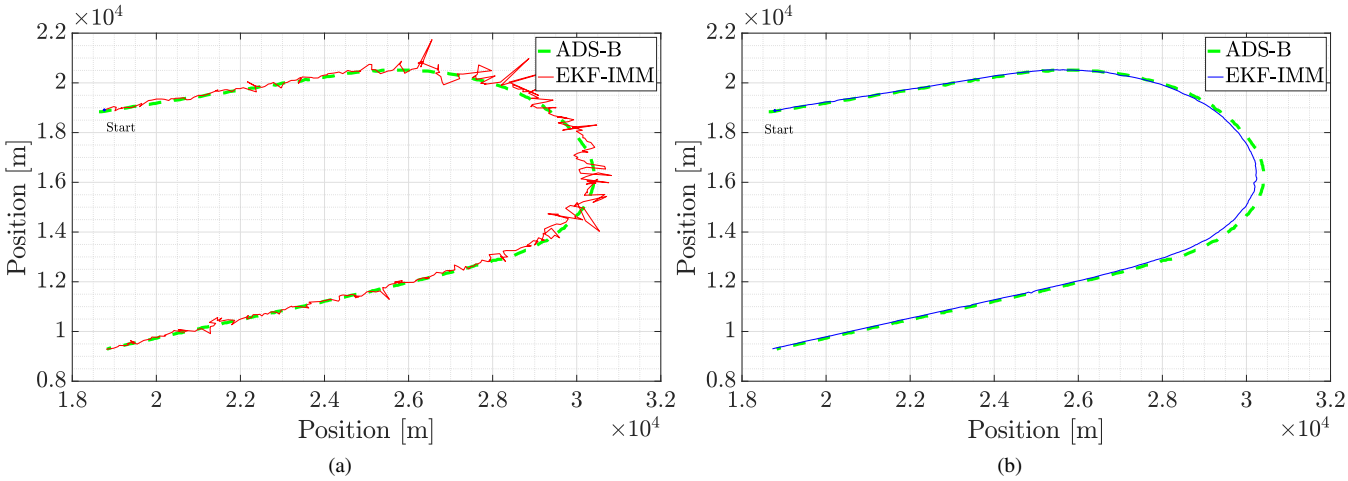

Fig. 6. Top view of estimated aircraft tracks during a turning trajectory. Comparison between the implemented IMM-based tracker and the ADS-B. (a) without outlier correction. (b) with outlier correction.

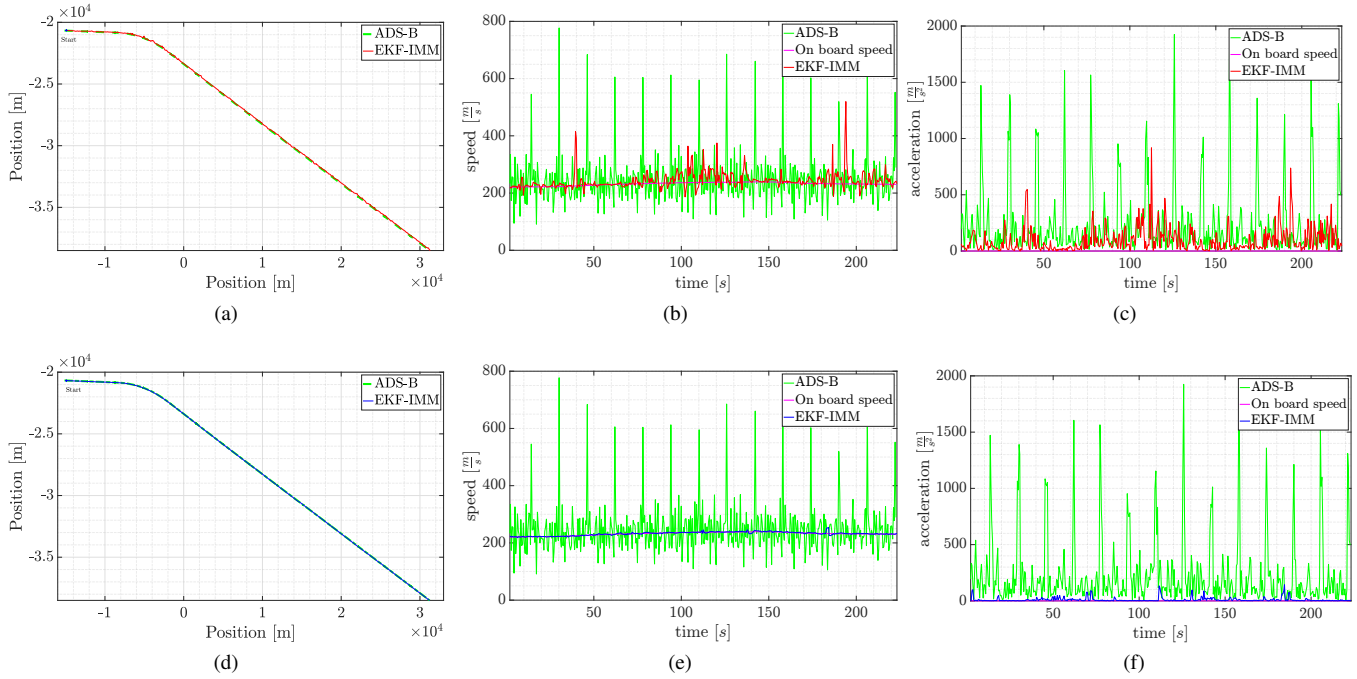

Fig. 7. Localization performance on the second aircraft trajectory. First row: comparison between the ADS-B (green) and IMM-based tracker without outlier correction (red), with on board computed horizontal speed and the corresponding derived horizontal acceleration (pink). (a) top view of $x-y$ position estimates, (b) horizontal speed, (c) horizontal acceleration. Second row: comparison between the ADS-B (green) and IMM-based trackers with outlier correction (blue), with on board computed horizontal speed and the corresponding derived horizontal acceleration (pink). (d) top view of $x-y$ position estimates, (e) horizontal speed, (f) horizontal acceleration.

with pink color the horizontal speed measured by an aircraft on board odometer in Fig. 7e, and the correspondent values of acceleration obtained by differentiation in Fig. 7f. This measurement should be used as reference comparison to assess the correctness of EKF-IMM estimate.

We first observe the noisy speed and acceleration estimates produced by the ADS-B. A similar trend is also present for the EKF-IMM tracker without outlier removal. Such sudden behaviors are clearly not compatible with an aircraft trajectory. On the other hand, discarding outliers leads to a smoother estimate of speed and acceleration. As a matter of fact, the aircraft shows an NCV behavior over time, as confirmed by the on board computed speed and also by the evolution of IMM model probabilities reported in Fig. 8, which suggest the high confidence of the NCV model for almost all the trajectory, except during the turn where the model likelihood of the CTR is prevalent (as it should be). The time interval associated to the turn is highlighted in light grey.

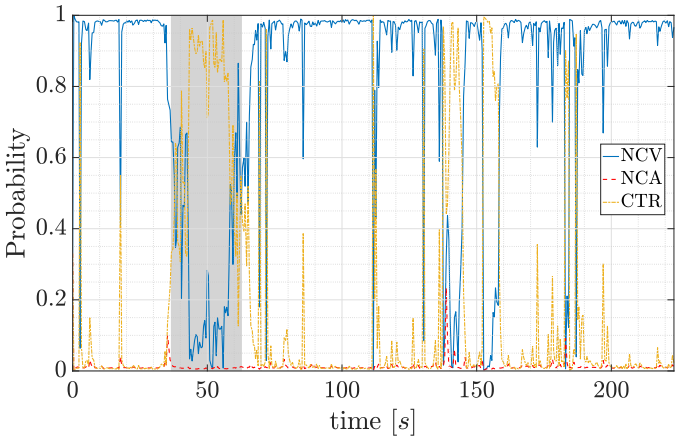

Fig. 8. Evolution of IMM model probabilities for the second aircraft trajectory. Grey area indicates the turning manoeuvring phase.

V. Conclusion

This work presented the results of an aircraft tracking application in a WAM scenario. The surveillance system refers to a network of GSs localizing airplanes by means of ranging information captured by Mode S messages around a main European airport. We perform aircraft tracking with an IMM-based filtering solution using three parallel EKFs, each calibrated according to a specific motion model to cope with different kinematics. To increase robustness, we developed an outlier identification and mitigation algorithm that discards unreliable measurements, allowing a faithful tracking system with performance compatible with the ADS-B positioning technology. The proposed method is shown to handle abrupt changes on trajectories, guaranteeing a smooth estimate (i.e., without abrupt variations) of the kinematic variables, especially for speed and acceleration. The results from real data demonstrate the benefits of the proposed algorithm over conventional approaches. Future developments should focus on analyzing the effect of acquiring angle of arrival (AOA) measurements, as well as the impact of more advanced algorithms for outlier mitigation or GS selection, or the hybridization with other localization technologies.

References

[1] "Performance review report 2022," Eurocontrol, Tech. Rep., 2022.

[2] T. Noskievič and J. Kraus, "Air traffic control tools assessment," *MAD-Magazine of Aviation Development*, vol. 5, no. 2, pp. 6–10, 2017.

[3] P. Brooker, "SEASAR and NextGen: investing in new paradigms," *The Journal of Navigation*, vol. 61, no. 2, pp. 195–208, 2008.

[4] "Guidance material on comparison of surveillance technologies (GMST)," ICAO, Tech. Rep., 2022.

[5] M. Strohmeier, M. Schäfer, V. Lenders, and I. Martinovic, "Realities and challenges of nextgen air traffic management: the case of ADS-B," *IEEE Communications Magazine*, vol. 52, no. 5, pp. 111–118, 2014.

[6] M. Arpaio, "An innovative perspective on ADS-B," in *2016 IEEE 2nd International Forum on Research and Technologies for Society and Industry Leveraging a better tomorrow (RTSI)*, 2016, pp. 1–4.

[7] M. Geyer and A. Daskalakis, "Solving passive multilateration equations using Bancroft's algorithm," in *17th DASC. AIAA/IEEE/SAE. Digital Avionics Systems Conference. Proceedings (Cat. No.98CH36267)*, vol. 2, 1998, pp. F41/1–F41/8 vol.2.

[8] M. Monteiro, A. Barreto, T. Kacem, J. Carvalho, D. Wijesekera, and P. Costa, "Detecting malicious ADS-B broadcasts using wide area multilateration," in *2015 IEEE/AIAA 34th Digital Avionics Systems Conference (DASC)*, 2015, pp. 4A3–1.

[9] G. Galati, M. Leonardi, P. Magaro, and V. Paciucci, "Wide area surveillance using SSR mode S multilateration: advantages and limitations," in *European Radar Conference, 2005. EURAD 2005.*, 2005, pp. 225–229.

[10] A. Filip-Dhaubhadel, M. A. Bellido-Manganell, T. Gräupl, and M. Schnell, "Feasibility assessment of LDACS-based wide area multilateration," in *2022 IEEE/AIAA 41st Digital Avionics Systems Conference (DASC)*, 2022, pp. 1–10.

[11] B. A. C. da Silva, P. P. Porto, and R. Eller, "Aeronautical surveillance systems: Historical and future perspectives," *Journal of the Brazilian Air Transportation Research Society*, vol. 9, no. 1, pp. 9–10, 2013.

[12] J. Naganawa, H. Miyazaki, and H. Tajima, "Localization accuracy model incorporating signal detection performance for wide area multilateration," *IEEE Transactions on Aerospace and Electronic Systems*, vol. 55, no. 4, pp. 1957–1971, 2019.

[13] S.-L. Jheng, S.-S. Jan, Y.-H. Chen, and S. Lo, "1090 MHz ADS-B-based wide area multilateration system for alternative positioning navigation and timing," *IEEE Sensors Journal*, vol. 20, no. 16, pp. 9490–9501, 2020.

[14] M. A. Garcia, R. Mueller, E. Innis, and B. Veytsman, "An enhanced altitude correction technique for improvement of WAM position accuracy," in *2012 Integrated Communications, Navigation and Surveillance Conference*, 2012, pp. A4–1–A4–9.

[15] G. Xiangmin, L. Renli, S. Hongxia, and C. Jun, "A survey of safety separation management and collision avoidance approaches of civil UAS operating in integration national airspace system," *Chinese Journal of Aeronautics*, vol. 33, no. 11, pp. 2851–2863, 2020.

[16] J. Tang, "Conflict detection and resolution for civil aviation: A literature survey," *IEEE Aerospace and Electronic Systems Magazine*, vol. 34, no. 10, pp. 20–35, 2019.

[17] H. Georgiou, S. Karagiorgou, Y. Kontoulis, N. Pelekis, P. Petrou, D. Scarlatti, and Y. Theodoridis, "Moving objects analytics: Survey on future location & trajectory prediction methods," *arXiv preprint arXiv:1807.04639*, 2018.

[18] H. Khaledian, R. Sáez, J. Vilà-Valls, and X. Prats, "Interacting multiple model filtering for aircraft guidance modes identification from surveillance data," *Journal of Guidance, Control, and Dynamics*, vol. 46, no. 8, pp. 1580–1595, 2023.

[19] E. J. Casado Magaña, "Trajectory prediction uncertainty modelling for air traffic management," Ph.D. dissertation, University of Glasgow, 2016.

[20] X. R. Li and V. P. Jilkov, "Survey of maneuvering target tracking: decision-based methods," in *Signal and Data Processing of Small Targets 2002*, vol. 4728. SPIE, 2002, pp. 511–534.

[21] H. Zhang, J. Xie, J. Ge, W. Lu, and B. Zong, "Adaptive strong tracking square-root cubature Kalman filter for maneuvering aircraft tracking," *IEEE Access*, vol. 6, pp. 10 052–10 061, 2018.

[22] A. Ellouze, M. Ksantini, F. Delmotte, and M. Karray, "Multiple object tracking: Case of aircraft detection and tracking," in *2019 16th International Multi-Conference on Systems, Signals & Devices (SSD)*, 2019, pp. 473–478.

[23] H. A. P. Blom, "An efficient filter for abruptly changing systems," in *The 23rd IEEE Conference on Decision and Control*, 1984, pp. 656–658.

[24] H. Blom and Y. Bar-Shalom, "The interacting multiple model algorithm for systems with Markovian switching coefficients," *IEEE Transactions on Automatic Control*, vol. 33, no. 8, pp. 780–783, 1988.

[25] E. Mazor, A. Averbuch, Y. Bar-Shalom, and J. Dayan, "Interacting multiple model methods in target tracking: a survey," *IEEE Transactions on aerospace and electronic systems*, vol. 34, no. 1, pp. 103–123, 1998.

[26] Y. Boers and J. N. Driessen, "Interacting multiple model particle filter," *IEE Proceedings-Radar, Sonar and Navigation*, vol. 150, no. 5, pp. 344–349, 2003.

[27] D. Musicki, R. Evans, and S. Stankovic, "Integrated probabilistic data association," *IEEE Transactions on Automatic Control*, vol. 39, no. 6, pp. 1237–1241, 1994.

[28] Y. Bar-Shalom, F. Daum, and J. Huang, "The probabilistic data association filter," *IEEE Control Systems Magazine*, vol. 29, no. 6, pp. 82–100, 2009.

[29] F. Meyer, T. Kropfreiter, J. L. Williams, R. Lau, F. Hlawatsch, P. Braca, and M. Z. Win, "Message passing algorithms for scalable multitarget tracking," *Proceedings of the IEEE*, vol. 106, no. 2, pp. 221–259, 2018.

[30] M. Brambilla, D. Gaglione, G. Soldi, R. Mendrzik, G. Ferri, K. D. LePage, M. Nicoli, P. Willett, P. Braca, and M. Z. Win, "Cooperative localization and multitarget tracking in agent networks with the sum-product algorithm," *IEEE Open Journal of Signal Processing*, vol. 3, pp. 169–195, 2022.

[31] B. Camajori Tedeschini, M. Brambilla, L. Barbieri, G. Balducci, and M. Nicoli, "Cooperative lidar sensing for pedestrian detection: data association based on message passing neural networks," *IEEE Transactions on Signal Processing*, vol. 71, pp. 3028–3042, 2023.

[32] B. Camajori Tedeschini, M. Brambilla, L. Barbieri, and M. Nicoli, "Addressing data association by message passing over graph neural networks," in *2022 25th International Conference on Information Fusion (FUSION)*, 2022, pp. 01–07.

[33] M. Brambilla, M. Nicoli, G. Soatti, and F. Deflorio, "Augmenting vehicle localization by cooperative sensing of the driving environment: insight on data association in urban traffic scenarios," *IEEE Transactions on Intelligent Transportation Systems*, vol. 21, no. 4, pp. 1646–1663, 2020.

[34] "CAT023 - EUROCONTROL specification for surveillance data exchange ASTERIX, part 16: Category 23, CNS/ATM ground station and service status reports," Eurocontrol, Tech. Rep., 2009.

[35] G. Rebane, "EASA basic regulation: improving the performance of the european aviation safety system," *ZLW*, vol. 68, p. 51, 2019.

[36] X. Rong Li and V. Jilkov, "Survey of maneuvering target tracking. Part I. Dynamic models," *IEEE Transactions on Aerospace and Electronic Systems*, vol. 39, no. 4, pp. 1333–1364, 2003.

[37] L. Johnston and V. Krishnamurthy, "An improvement to the interacting multiple model (IMM) algorithm," *IEEE Transactions on Signal Processing*, vol. 49, no. 12, pp. 2909–2923, 2001.